EFFICIENT FFT METHOD FOR MODELLING PERFORMANCE OF RADARS WITH SCAN-TO-SCAN FEEDBACK INTEGRATION

Josef Zuk

DSTO, Australia
E-Mail: josef.zuk@dsto.defence.gov.au

Luke Rosenberg

DSTO, Australia
University of Adelaide, Australia

ABSTRACT

In discrete-event simulation (DES) involving radar systems, one is concerned with tracking the evolution of detection probability as explicitly simulated successive scans elapse. The survival-function based FFT technique discussed here constitutes an improvement over a previously developed approach, that provides speed and efficiency in maintaining and updating the detection state, and likewise for extracting the detection probability from the state after any scan over the target. It is shown to be particularly useful for modelling high-resolution airborne maritime surveillance radars that employ a combination of range stretching and autoregressive scan-to-scan integration.

Index Terms— Radar detection, Autoregressive processes, Fast Fourier transforms.

1. INTRODUCTION

Fast executing software models of radar performance are essential in many applications, especially as components within constructive and human-in-the-loop simulations for operational studies of air combat and surveillance, where overall computational efficiency is a stringent requirement. This is especially relevant for complex detection schemes as seen in high-resolution airborne maritime surveillance radars that employ a combination of range stretching and autoregressive scan-to-scan integration, such as the AN/APS-134 family [1, 2].

Fast Fourier transform (FFT) techniques are suited to such problems, and are generally applied to the probability density function (PDF) of returned power, which leads to a formulation in terms of the characteristic function, while the state of the system between updates (*i.e.* successive scans) is maintained via the discretized PDF [3]. (See also [4, 5].) In the present work, an FFT method is applied to the survival function — synonymous with the complementary cumulative distribution function (CDF), and the system state is stored as a finite sequence of its Fourier coefficients. The detection probability after any number of scans can be computed directly and explicitly from these, which eliminates a significant bottleneck relative to the standard approach, as it avoids applying the inverse FFT to recover the PDF, followed by its subsequent integration in order to read the detection probability from the CDF.

The effects of range stretching are easily expressed in terms of the survival function, whereas the associated PDF is a cumbersome quantity. The effects of power-level saturation are also conveniently incorporated into the survival function.

2. SYSTEM DESCRIPTION

In a high-resolution radar, the number of range gates (micro range-resolution cells) far exceeds the number of pixels available to represent the maximum range extent of the radar display. Range stretching aggregates the returned power from K micro cells into a single statistic (assumed here to be the maximum) that is then associated with a single macro cell. Macro cells map onto the display pixels on which detection decisions are based. The number of micro cells per macro cell K is called the stretch factor.

The power level Z associated with each macro cell is stored in digital memory, and is updated once per scan period by means of the autoregressive Markov law

$$Z_n = \beta Z_{n-1} + X_n \ , \tag{1}$$

where $n = 1, 2, \ldots$ counts successive scans, and $0 \ll \beta < 1$ is a feedback constant. The formal solution after n scans may be expressed as a discounted sum in powers of β [6]. The innovations X_n, which represent the returned power from the target and interference after range stretching, are assumed to be independent and identically distributed random variables (RV). Let $f(x)$ denote the common PDF of the innovations X_n, and $\phi_n(z)$ the PDF of the output after n scans, with $F(x), \Phi_n(z)$ their respective CDFs. An over-bar will signify the survival function, while a tilde will indicate a Fourier transform. The state-update equation for the PDF is

$$\phi_n(z) = \int_{-\infty}^{\infty} dy\, f(z - \beta y)\phi_{n-1}(y) \ , \tag{2}$$

with a steady-state distribution $\phi_{\rm ss}(z)$ approached as $n \to \infty$. The Fourier-space version of the state-update equation asserts that the characteristic function satisfies

$$\tilde{\phi}_n(k) = \tilde{f}(k)\tilde{\phi}_{n-1}(\beta k) \ . \tag{3}$$

The treatment of the detection problem in [3] was based on this formulation. One may observe that explicit iteration of (3) yields the product form

$$\tilde{\phi}_n(k) = \tilde{\phi}_0(\beta^n k) \cdot \prod_{\ell=0}^{n-1} \tilde{f}(\beta^\ell k) \ , \tag{4}$$

relating to an assumed initial distribution $\phi_0(z)$.

The combination of a compound clutter K-distribution [7] with range stretching leads to innovations that are sufficiently complex to make the autoregressive problem difficult to treat analytically. This is further complicated by spatial correlation of the clutter radar cross-section (RCS) which may be significant over many micro range cells [8]. We consider the two limiting cases of perfect correlation among

the micro cells comprising a macro cell ('long' model), and no correlation ('short' model). The building block for the innovation CDF is a function $F_{K,T}(x;S)$ given in [6] that depends on the clutter shape parameter ν and clutter-to-noise ratio (CNR) c, in addition to the signal-to-interference ratio (SIR) S and radial target extent measured in micro cells T. Both S and the returned power x are measured here in units of the mean micro-cell interference, while c is measured with respect to mean micro-cell thermal noise. For the 'long' model, the innovation CDF is simply $F(x;S) = F_{K,T}(x;S/T)$, while for the 'short' model it is constructed as

$$F(x;S) = [F_{1,0}(x;0)]^{K-T} \cdot [F_{1,1}(x;S/T)]^{T} \ . \tag{5}$$

A uniform partitioning of target RCS has been assumed. Setting $S \equiv 0$ yields the interference-only distributions. It should be noted that the present method will work for any non-negative innovation X provided it has finite mean.

Determination of the threshold level $z_{\rm b}$ from the desired probability of false alarm $P_{\rm FA}$ has been discussed in [6], where a rare-event Monte Carlo (MC) technique was invoked. In order to decouple the present discussion from considerations of the (non-trivial) relationship between threshold and false-alarm rate, we shall regard the detection probability as a function of the threshold level, parametrized by the SIR: $P_{\rm D}(z_{\rm b}) = \bar{\Phi}(z_{\rm b};S)$, rather than the opposite as is typically the case in radar performance analysis.

3. FOURIER TRANSFORM TECHNIQUE

In a practical system, the RV Z will be linearly transformed and quantized into discrete greyscale levels corresponding to illumination intensity on the radar display. Since the illumination that the display can support is necessarily bounded, it should be clear that arbitrarily large returned power cannot be represented faithfully. Returns above the maximum power level will saturate at the highest greyscale level. We take account of this by introducing an explicit saturation power level expressed as a constant multiple of the mean output interference power. This is an appropriate choice because we also assume that the automatic gain control (AGC) system acts to drive all interference-only pixel illumination levels to a globally constant local mean value which, without loss of generality, may be set to unity. Thus, while the pixel illumination variance may vary between different regions of the display, the mean remains constant.

In view of the foregoing remarks, it is convenient to work with a renormalized unit-gain version of the AR(1) process:

$$Z'_n = \beta Z'_{n-1} + (1-\beta)X'_n \ , \tag{6}$$

with $X' \equiv X/\mu_{\rm str}$, where $\mu_{\rm str}$ is the interference-only innovation mean, *i.e.* the mean macro-cell interference power measured in units of the mean micro-cell interference. The variance $\sigma^2_{\rm str}$ is similarly interpreted. For the 'long' model, there are closed analytic expressions for $\mu_{\rm str}$ and $\sigma^2_{\rm str}$ while, for the 'short' model, they are easily estimated via Gaussian quadrature, or from extreme value theory (EVT) provided K is sufficiently large. This recasting of the feedback relation merely comprises a change in normalization given by $Z' = (1-\beta)Z/\mu_{\rm str}$, and has the effect of giving Z' unit mean in the interference-only steady state, $\langle Z'_{\rm ss}\rangle = 1$. The configuration-space state-update equation for the PDF now becomes

$$\phi_n(z) = \frac{1}{\beta(1-\beta)} \int_{-\infty}^{+\infty} dy\, f\left(\frac{z-y}{1-\beta}\right) \phi_{n-1}\left(\frac{y}{\beta}\right) \ , \tag{7}$$

and the analogue of Eq. (3) is

$$\tilde{\phi}_n(k) = \tilde{f}\left((1-\beta)k\right) \tilde{\phi}_{n-1}(\beta k) \ . \tag{8}$$

Power-level saturation is implemented by truncating the survival function of the innovation at a cut-off $x_{\rm c}$, *i.e.* setting $\bar{F}(x) \equiv 0$ for all $x > x_{\rm c}$. In a practical system, this is achieved by using less bits to transmit the innovation data than is used to store and manipulate the pixel data. Introducing $\lambda \equiv \bar{F}(x_{\rm c})$, we can write

$$\bar{F}(x) = (1-\lambda)G(x) + \lambda\Theta(x_{\rm c} - x) \ , \tag{9}$$

where $\Theta(x)$ is the Heaviside step function, while for $x \le x_{\rm c}$

$$G(x) \equiv 1 + \left(\bar{F}(x) - 1\right)/(1-\lambda) \ , \tag{10}$$

and is zero for $x > x_{\rm c}$. $G(x)$ is also a valid survival function.

In general, a survival function tends to unity as its argument approaches negative infinity. However, since we are considering explicitly non-negative random variables (*viz.* power values), we may deal with a survival function restricted to the semi-infinite positive real line, and extended with zero values along the negative half-line. Furthermore, the physical requirement that the mean power be finite guarantees the existence of a well-defined Fourier transform for the survival function. By definition,

$$\bar{F}^+(x) \equiv \begin{cases} \bar{F}(x) & \text{for} \quad x \ge 0 \\ 0 & \text{for} \quad x < 0 \end{cases} \ , \tag{11}$$

and similarly for $G^+(x)$ and $\bar{\Phi}^+(z)$.

Eq. (7) implies that $\bar{\Phi}^+(z)$ is updated after a single scan according to

$$\bar{\Phi}^+(z) \leftarrow \bar{F}^+\left(\frac{z}{1-\beta}\right) + \frac{1}{1-\beta}\int_{-\infty}^{+\infty} dy\, f\left(\frac{z-y}{1-\beta}\right) \bar{\Phi}^+\left(\frac{y}{\beta}\right) . \tag{12}$$

For the Fourier transform of $\bar{\Phi}^+(z)$, it follows that

$$\tilde{\bar{\Phi}}(k) \leftarrow \beta\tilde{\bar{\Phi}}(\beta k) + \left[1 - i\beta k\tilde{\bar{\Phi}}(\beta k)\right] \cdot (1-\beta)\tilde{\bar{F}}((1-\beta)k) \ , \tag{13}$$

where we have related the Fourier-space PDF with the Fourier-space survival function according to $\tilde{f}(k) = 1 - ik\tilde{\bar{F}}(k)$. Observing that

$$\tilde{\bar{F}}(k) = (1-\lambda)\tilde{G}(k) + \lambda x_{\rm c} e^{-ikx_{\rm c}/2}\,\mathrm{sinc}\,(kx_{\rm c}/2) \ , \tag{14}$$

we obtain, in terms of G^+, the final state-update equation

$$\begin{aligned} \tilde{\bar{\Phi}}(k) \leftarrow{}& \beta\tilde{\bar{\Phi}}(\beta k) + (1-\beta)\left[1 - i\beta k\tilde{\bar{\Phi}}(\beta k)\right] \\ &\times \Big[(1-\lambda)\tilde{G}((1-\beta)k) \\ &+ \lambda x_{\rm c} e^{-i(1-\beta)kx_{\rm c}/2}\,\mathrm{sinc}\,((1-\beta)kx_{\rm c}/2)\Big] \ . \end{aligned} \tag{15}$$

We represent the innovation in terms of the Fourier coefficients for G^+ as they are free of discontinuity at the upper edge.

4. THE DISCRETIZED PROBLEM

Because of power-level saturation, the system detection state has finite extent, and due to the quantization of returned power into discrete greyscale levels, it has finite resolution (so that its spectrum has finite extent). Hence, the survival functions are well-suited to spectral decomposition in terms of a finite collection of discrete wavenumbers $k_\mu = \mu\Delta k$ via the discrete Fourier transformation (DFT). For the innovation,

$$G^+(x) = \frac{1}{N}\sum_{\mu=0}^{\pm(N-1)/2} A_\mu e^{i\mu\Delta k\cdot x} \ , \tag{16}$$

for N odd. Since $G(x)$ is real-valued, the spectral coefficients satisfy $A_{-\mu} = A_\mu^*$, yielding $(N+1)/2$ complex degrees of freedom. While $G^+(x)$ is originally defined on a bounded symmetric interval $-L/2 \le x \le +L/2$ (albeit identically zero on the negative branch), the series (16) represents $G^+(x)$ by an extension that is necessarily periodic. Imposing the minimal condition $G^+(x+L) = G^+(x)$ implies a wave-number spacing $\Delta k = 2\pi/L$. For the problem at hand, $L = 2x_\mathrm{c}$. Sampling $G^+(x)$ at $x \equiv m\Delta x$ for $m = 0, 1, \ldots, (N-1)/2$, with spacing $\Delta x = L/N = 2\pi/(N\Delta k)$, allows us to write

$$A_\mu = \sum_{m=0}^{(N-1)/2} G^+(m\Delta x) e^{-2\pi i \mu m/N} \ . \tag{17}$$

The number of points N contributing to the DFT is regarded as *a priori* undetermined, to be computed so as to achieve a given desired configuration-space resolution. For this purpose, the required resolution expressed as a fraction of significant function extent ρ is introduced. The absolute resolution is then $\delta x = \rho L/2$. For example, if the number of greyscale levels is the standard 256, then one would set $\rho \lesssim 0.005$. We shall oversample by a factor ξ, and ultimately apply a low-pass filter (in the form of a Gaussian sliding window) to re-instate a resolution of δx. The role of the oversampling factor is to determine the window width, whose value should ensure sufficient damping of sidelobe oscillations. The required unpadded (odd) number of sample points N to achieve the required degree of oversampling is

$$N = 2\,\mathrm{ceil}(\xi L/(2\delta x)) - 1 \ . \tag{18}$$

However, in order to apply the FFT, the spectrum must be zero-padded with an additional $1 \le \Delta N < N$ points to bring the total sample points to a power of two. With $N' \equiv N + \Delta N$, we observe that the minimum required number of zero-padded sample points is

$$N' = 2^{\mathrm{ceil}(\log_2(N))} \ . \tag{19}$$

Accordingly, we resample at the points $x \equiv m\Delta x'$, with the new spacing $\Delta x' = L/N'$, which enables us to write

$$G^+(m\Delta x') = \frac{1}{N'} \sum_{\mu=0}^{N'-1} B_\mu e^{2\pi i m\mu/N'} \ , \tag{20}$$

having introduced the FFT spectral coefficients

$$(N/N')B_\mu \equiv \begin{cases} A_\mu & \text{for} \quad \mu = 0, 1, \ldots, \frac{1}{2}(N-1) \ , \\ 0 & \text{for} \quad \mu = \frac{1}{2}(N+1), \ldots, N' - \frac{1}{2}(N+1) \ , \\ A^*_{N'-\mu} & \text{for} \quad \mu = N' - \frac{1}{2}(N-1), \ldots, N'-1 \ . \end{cases} \tag{21}$$

We also introduce

$$G_m \equiv \begin{cases} G^+(m\Delta x') & \text{for} \quad 0 \le m \le L/(2\Delta x') \ , \\ 0 & \text{for} \quad L/(2\Delta x') < m \le N'-1 \ . \end{cases} \tag{22}$$

Collecting the B_μ and G_m into N'-dimensional column vectors, we obtain the FFT pair

$$\mathbf{B} = \mathrm{FFT}_{N'}(\mathbf{G}) \ , \quad \mathbf{G} = \mathrm{IFFT}_{N'}(\mathbf{B}) \ . \tag{23}$$

The spectral coefficients A_μ are recovered as N/N' times the first $(N+1)/2$ elements of the vector $\mathbf{B}$.

It is advantageous to trade zero-padding for oversampling. In particular, we minimize ΔN to unity by upwardly revising N to $N = N' - 1$ with N' given by Eq. (19), and then compensating the ensuing finer sample spacing by increasing the oversampling to $\xi \mapsto (N+1)\delta x/L$, which ensures that the desired resolution remains fixed at δx. In practice, it suffices to choose an initial value of $\xi = 2$, which establishes the minimum level of oversampling.

The Fourier-space state-update equation requires not $\tilde{G}(k_\mu)$ but the interpolated values $\tilde{G}((1-\beta)k_\mu)$. Provided the feedback parameter has the form $\beta = 1 - 1/2^b$, with $b = 0, 1, 2, \ldots$ (not a significant restriction when one considers potential digital implementations of the feedback integrator), these may be extracted by appealing to further zero-padding. The FFT size $N_\mathrm{fft} = N'/(1-\beta) = 2^b \cdot N'$ allows extraction of the interpolated values and provides sufficient zero-padding to avoid aliasing problems.

If the innovation CDF $F(x)$ is sampled at $F_m = F(m\Delta x')$, then the survival function sampling is given by

$$G_m = \begin{cases} 1 - F_m/(1-\lambda) & \text{if} \quad m\Delta x' \le x_\mathrm{c} \ , \\ 0 & \text{if} \quad m\Delta x' > x_\mathrm{c} \ . \end{cases} \tag{24}$$

Once the vector $\mathbf{G}$ is zero-padded to length N_fft, and the FFT applied to give $\mathbf{B} = \mathrm{FFT}_{N_\mathrm{fft}}(\mathbf{G})$, then the discretized input to the state-update equation at $k = \mu\Delta k$ $(0 \le \mu \le (N-1)/2)$ is obtained as

$$\tilde{G}((1-\beta)\Delta k{\cdot}\mu) = B_\mu{\cdot}\Delta x' \ . \tag{25}$$

We must also extract the interpolated Fourier-space survival function $\tilde{\bar{\Phi}}(\beta\Delta k{\cdot}\mu)$ from the current stored detection state

$$\{\mathcal{A}_\mu \equiv \tilde{\bar{\Phi}}(\Delta k{\cdot}\mu) : \mu = 0, 1, \ldots, (N-1)/2\} \ . \tag{26}$$

An exact interpolation necessitates invocation of the sinc-interpolation formula (recalling $\mathcal{A}_{-\mu} = \mathcal{A}_\mu^*$):

$$\tilde{\bar{\Phi}}(\beta\Delta k{\cdot}\mu) = \sum_{\nu=0}^{\pm(N-1)/2} \mathcal{A}_\nu \,\mathrm{sinc}\,(\pi(\nu - \beta\mu)) \ . \tag{27}$$

Unfortunately, this is excessively computationally intensive. Approximate linear and spline interpolation schemes perform adequately over a few scans, but quickly build up significant error as the number of iterations grows. A tractable alternative is to use a zero-padded FFT/IFFT pair to emulate the sinc-interpolation, which proceeds as follows: The vector of $(N+1)/2$ Fourier coefficients that stores the current detection state $\mathcal{A}$ is transformed into a vector $\mathcal{B}$ of length N' as in Eq. (21). The IFFT is applied to $\mathcal{B}$, and the resulting vector is zero-padded to 2^b times its original length (*viz.* N_fft). The FFT is then taken, and the elements corresponding to indices $(2^b - 1)\mu$ are extracted for $\mu = 0, 1, \ldots, (N-1)/2$. The resulting vector has length $(N+1)/2$ and yields the desired interpolation $\tilde{\bar{\Phi}}(\beta\Delta k{\cdot}\mu)$. This process is aided by use of the built-in MATLAB function `interpft`.

In principle, one could recover the entire survival function on a discrete grid via an IFFT, and then employ a suitable interpolation scheme to read off the detection probability associated with *any* threshold level. But this is superfluous for many performance analysis applications (such as DES) where it is appropriate to work with a fixed mean time between false alarms. In this case, after any given scan, the detection probability is required only for a single predetermined threshold z_b, which can be computed directly from the Fourier state coefficients by means of a DFT reconstruction formula:

$$P_\mathrm{D}(z_\mathrm{b}) = \frac{\Delta k}{2\pi}\Big\{\mathcal{A}_0 + 2 \sum_{\mu=1}^{(N-1)/2} w_\mu \left[\Re(\mathcal{A}_\mu)\cos(\mu\Delta k{\cdot}z_\mathrm{b}) - \Im(\mathcal{A}_\mu)\sin(\mu\Delta k{\cdot}z_\mathrm{b})\right]\Big\} \ . \tag{28}$$

The Gaussian sliding window has been applied here by means of the Fourier weights

$$w_\mu = \exp\left[-\left(\pi\xi/k_{\rm g}N\right)^2\mu^2\right] \ , \tag{29}$$

where $k_{\rm g} \equiv 2\sqrt{\ln 2}$. This eliminates unwanted ripple that would be particularly noticeable on the flat part of the detection curve and, more significantly, ringing due to the step at the origin, near which (up to some multiple of $\Delta x'$), one should also impose $P_{\rm D}(z) \equiv 1$ in order to counteract the natural tendency for $P_{\rm D}(z)$ to approach $1/2$ as $z \to 0^+$ [9].

5. RESULTS

While the method works for any initial pixel distribution, we are interested in integrating a given pixel (representing a fixed surface patch) which, at time zero, is in the interference-only steady state, having been under observation over a long period. At this time, the pixel becomes occupied by a target with SIR S. This may be a pop-up such as a submarine periscope or the result of target motion. We approximate the initial steady-state distribution by the Gaussian form of the applicable central limit theorem (CLT) [10, 11]. This is valid as the tails of the distribution are not important. The relevant discretized Gaussian characteristic function is given by

$$\tilde{\phi}_\mu = e^{-i\mu_{\rm pix}k_\mu}\cdot e^{-\sigma^2_{\rm pix}k^2_\mu/2} \ , \tag{30}$$

with

$$\mu_{\rm pix} \equiv 1 \ , \quad \sigma^2_{\rm pix} = \frac{1-\beta}{1+\beta}\cdot\left(\frac{\sigma_{\rm str}}{\mu_{\rm str}}\right)^2 \ . \tag{31}$$

The initial Fourier-space survival function is then derived as

$$\mathcal{A}_\mu = \begin{cases} \mu_{\rm pix} & \text{for} \quad \mu = 0 \ , \\ (1-\tilde{\phi}_\mu)/(ik_\mu) & \text{for} \quad \mu \neq 0 \ . \end{cases} \tag{32}$$

In any case, the state may be iterated for a number of scans with interference-only innovations in order to achieve a more precisely determined steady state.

We present results for both the 'long' and 'short' models, and compare these with Monte Carlo simulations. We consider a system defined by $x_{\rm c} = 10$, $\rho = 0.005$, which gives an FFT size of $N' = 1024$. The remaining system, target and environmental parameters are set as in Table 1.

Table 1. Modelling parameters

Quantity	Symbol	Value
Feedback parameter	β	$15/16$
Stretch factor	K	10
Clutter shape parameter	ν	1
Clutter-to-noise ratio	c	1000
Signal-to-interference ratio	S	10
Target extent	T	1

In Figs (1) and (2), the output survival functions are plotted for increasing numbers of scans up to $n = 300$ (by which time the steady state has set in) for the 'long' and 'short' models, respectively. The MC results coincide identically with their respective computed curves. Typical threshold levels are indicated ($z_{\rm b} = 2.80$ and 2.23 for the 'long' and 'short' models, respectively), based on $P_{\rm FA} = 10^{-6}$ [6]. One can track the increase in detection probability towards its steady-state level by the intercepts with the threshold

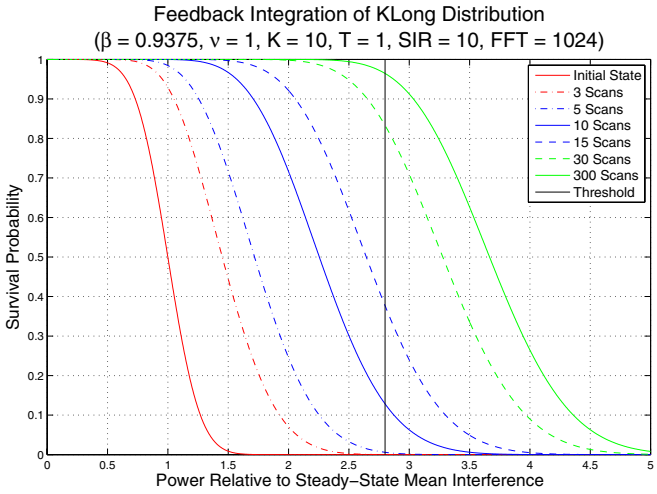

Fig. 1. Survival function versus normalized power for the 'long' model

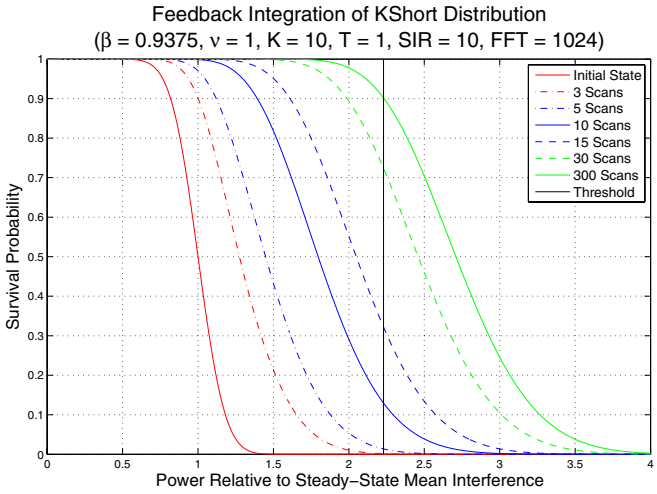

Fig. 2. Survival function versus normalized power for the 'short' model

line. The two models exhibit quite similar detection performance in this case [3].

In the present iterative approach, one may drop the assumption that the SIR remains constant between scans, *i.e.* the innovations X_n are not required to be identically distributed in the presence of a target. This facilitates performance analysis in operationally realistic dynamic scenarios.

6. CONCLUSIONS

For radar systems employing autoregressive scan-to-scan integration, we have derived an equation for efficiently iterating the detection state, stored as discrete Fourier coefficients $\mathcal{A}_\mu$ of the survival function for the display pixel power distribution, from which the probability of detection after a given scan follows directly. The formalism is particularly convenient for systems that also implement range stretching.

7. REFERENCES

[1] J.M. Smith, "AN/APS-134(V) maritime surveillance radar," in *Radar 82: Proceedings of the International Conference*, Oct. 1982, pp. 36–40.

[2] J.J. Ousborne, D. Griffith, and R.W. Yuan, "A periscope detection radar," *John Hopkins APL Technical Digest*, vol. 18, no. 1, pp. 125–133, 1997.

[3] L. Rosenberg and J. Zuk, "Performance prediction modelling for high resolution radar with scan-to-scan processing," in *2014 IEEE Radar Conference*, Cincinnati, OH, USA, May 2014, pp. 365–370.

[4] N. Letzepis and A.G. Fàbregas, "Outage analysis in MIMO free-space optical channels with pulse-position modulation," Technical Report CUED/F-INFENG/TR 597, Department of Engineering, University of Cambridge, UK, Feb. 2008.

[5] N. Letzepis and A.G. Fàbregas, "Outage probability of the Gaussian MIMO free-space optical channel with PPM," *IEEE Trans. Commun.*, vol. 57, no. 12, pp. 3682–3690, 2009.

[6] J. Zuk and L. Rosenberg, "Rare-event simulation for radar threshold estimation in heavy-tailed sea clutter," in *IEEE Workshop on Statistical Signal Processing 2014*, Gold Coast, Queensland, Australia, June 2014.

[7] K.D. Ward, R.J.A. Tough, and S. Watts, *Sea Clutter: Scattering, the K-Distribution and Radar Performance*, The Institute of Engineering Technology, London, UK, 2006.

[8] S. Watts, "Cell-averaging CFAR gain in spatially correlated K-distributed clutter," in *IEE Proceedings on Radar, Sonar and Navigation*, 1996, vol. 143, pp. 321–327.

[9] J.W. Brown and R.V. Churchill, *Fouries Series and Boundary Value Problems*, McGraw-Hill Inc, New York, USA, fifth edition, 1993, Section 19.

[10] H.U. Gerber, "The discounted central limit theorem and its Berry-Esséen analogue," *The Annals of Mathematical Statistics*, vol. 42, no. 1, pp. 389–392, 1971.

[11] W. Whitt, "Stochastic Abelian and Tauberian theorems," *Zeitschrift für Wahrscheinlichkeitstheorie und Verwandte Gebiete*, vol. 22, no. 4, pp. 251–267, 1972.